A New Analog Predistortion Criterion with Application to High Efficiency Digital Radio Links

Maria-Gabriella Di Benedetto, *Senior Member, IEEE,* and Paolo Mandarini

Abstract—**This paper describes a new approach for designing analog cubic predistorters in view of minimizing non linear distortion introduced by the high power amplifier (HPA) in microwave radio links.**

The approach is based on a global mean squared error minimization between the input to the predistorter and the output of the power amplifier, rather than on the elimination of the cubic term. In this manner, two advantages are obtained. Firstly, the off-band distortion terms are reduced so that it is possible to eliminate the HF transmission filter. Secondly, the interference produced by the nonlinear distortion can be uniformly distributed over the entire constellation so that it is possible to reduce the back-off value of the HPA.

Results of the application of the method proposed to some high spectrally efficient QAM systems, such as the 512-QAM system, are presented.

I. Introduction

THE POWER amplifiers (HPA) in microwave radio systems are characterized by instantaneous non linear distortions [1]. Consequently, they produce a widening of the power spectral density of the transmitted signal, obliging the use of strict RF filtering to avoid interferences on adjacent channels, and thus non linear intersymbol interference with memory. This last effect cannot be recovered easily by the receiver by means of fixed or adaptive equalizers.

Three strategies have been proposed to limit the aforementioned negative effects. They consist of controlling either the constellation before the modulator [data predistortion], or the received signal [non linear equalization], or the modulated signal (at Intermediate Frequency IF or Radio Frequency RF) before the power amplifier [analog predistortion].

The first technique [2] and [3] is appropriate for adaptive realizations and consists in generating a predistorted constellation, which, after modulation and amplification in the HPA, gives rise to the desired constellation. However, this method does neither allow the control of the overall transmitted power spectral density nor the reduction of the amount of non linear distortion introduced, and thus does not seem applicable to high efficiency systems. The control of the transmitted power spectral density is impossible also in recent versions of this method in which the predistortion of the constellation is made dependent upon preceding or succeeding symbols (data predistortion with memory [19], [21], or the predistortion is controlled several times within the symbol interval (data predistortion using interpolation [20]).

The second method [4] and [5] gives rise to highly complex systems, located at the receiver.

The third method [6] and [7] consists in inserting at IF or RF (before the power amplifier), a memoryless non linear predistortion (usually of the third order) on the signal which should compensate for the third order component introduced by the power amplifier. This procedure gives rise to good results for systems with a high number of levels, without introducing a high complexity [8]. However, an adaptive version of this system implies a processing concentrated in the power amplifier which can limit its use in satellite systems [9]. Methods which reduce the third-order component have been given particular attention. However, in the case of high spectral efficiency systems, this choice does not seem to be appropriate. In fact, in order to obtain sufficient margins against fading the power amplifiers are used close to the saturation point making the procedures based on the power series development not valid. Consequently, the preceding strategy does not lead to good control of all the off-band distortion terms, and the use of filtering of the signal at RF is required, with the effect of provoking, together with the non linearity, a dispersion of the constellation which cannot be recovered by the adaptive equalizer in the receiver.

In this paper, a different criterion for analog predistortion, which will be called MMSE criterion, will be presented. This method still considers the use of a cubic predistorter, but it is based on a global mean squared error minimization between the input to the predistorter and the output of the power amplifier, rather than on the elimination of the cubic term.

The present paper is organized as follows. In Section II, the method for calculating the coefficients of the predistorter and the performance of this method in the case of QAM modulation schemes will be presented. In Section III, the analysis will be applied to the case of a terrestrial radio link at 2 × 155 Mb/s and channel step of 40 MHz. Section IV is dedicated to the conclusions.

In what follows, potentially complex parameters and functions will be indicated in bold letters.

Paper approved by M. J. Joindot, the Editor for Radio Communications of the IEEE Communications Society. Manuscript received July 1, 1992; revised September 1, 1992, December 22, 1992, and February 2, 1995. This work was supported by Fondazione Ugo Bordoni.

The authors are with the Dipartimento INFOCOM-Università di Roma 'La Sapienza,' 00184 Rome, Italy.

IEEE Log Number 9414781.

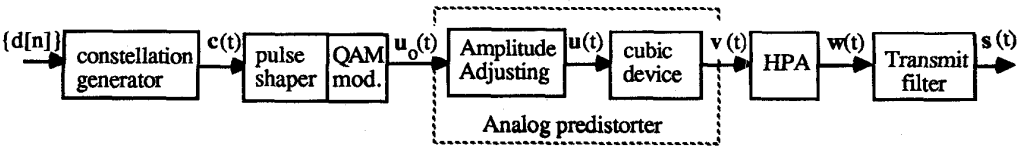

Fig. 1. Block diagram of the transmitter in a QAM system.

TABLE I
RELATION BETWEEN M AND L PARAMETERS IN THE CASES EXAMINED IN THE PRESENT STUDY

L value	Corresponding M value
128	12
256	18
512	26

II. DEFINITION AND PERFORMANCE OF THE MMSE PREDISTORTER

A. Definition of the MMSE Predistorter

Fig. 1 shows the block diagram of a transmitter in a QAM system. It is supposed that the sequence of complex data $\{d[n]\}$ can take on L values. The symbol frequency is indicated by f_c.

The coder generates, for each symbol, a point of a constellation which is approximately contained in a circle. This type of constellation, contrary to those more commonly used which are contained in a square, leads to a more efficient use of the final amplifier. In particular, the coder associates to each symbol $d[n]$ a pair of numerical values $\{x[n], y[n]\}$ each belonging to a set of $M = M(L)$ values, uniformly distributed between -1 and 1. Table I shows the relation between M and L in the cases of the present study.

The pulse shaper generates the two components $x(t)$ and $y(t)$, expressed as

$$x(t) = \sum_k x[k]g(t - kT_c) \tag{1}$$

$$y(t) = \sum_k y[k]g(t - kT_c). \tag{1'}$$

Two cases will be considered. In the first case, the data pulse $g(t)$ is a raised-cosine with roll-off factor γ

$$g(t) \leftrightarrow \mathbf{G}(f) = \mathbf{G}_\gamma(f)/f_c \quad \text{(case A)} \tag{2}$$

$$\mathbf{G}_\gamma(f) = \begin{cases} 1 & |f| \le \frac{f_c}{2}(1-\gamma) \\ \frac{1}{2}\left[1 - \sin\frac{\pi}{\gamma f_c}(f - f_c/2)\right] & \frac{f_c}{2}(1-\gamma) \le |f| \le \frac{f_c}{2}(1+\gamma) \\ 0 & \text{elsewhere.} \end{cases} \tag{2'}$$

In the second case, the preceding shaping is equally divided between the transmitter and the receiver

$$g(t) \leftrightarrow \mathbf{G}(f) = \sqrt{\mathbf{G}_\gamma(f)}/f_c \quad \text{(case B).} \tag{2''}$$

The modulated signal is represented by its normalized complex envelope

$$\mathbf{u}_0(t) = x(t) + jy(t). \tag{3}$$

Supposing that the emitted symbols are statistically independent, the power spectral density and the average power of $\mathbf{u}_0(t)$ are

$$\mathcal{P}_{\mathbf{U}_0}(f) = \mathcal{P}_c \cdot f_c \cdot |\mathbf{G}(f)|^2 \tag{4}$$

$$\mathcal{P}_{\mathbf{U}_0} = \mathcal{P}_c \cdot f_c \int_{-\infty}^{\infty} |\mathbf{G}(f)|^2 df \tag{4'}$$

where, in the present case of circular constellations

$$\mathcal{P}_c = \overline{\{x^2[k] + y^2[k]\}} \cong \frac{\pi}{6}\frac{M+1}{M-1}. \tag{4''}$$

Here and in the following, $\overline{(\,)}$ will indicate the ensemble average.

Indicating by B_{dB} the input back-off factor and by $W_{\mathbf{U}_0}$ the maximum instantaneous power of $\mathbf{u}_0$, the "amplitude adjusting device" (see Fig. 1) multiplies $\mathbf{u}_0(t)$ by $\alpha = 10^{B_{\text{dB}}/20}/\sqrt{W_{\mathbf{U}_0}}$, in order to limit the amplitude to the maximum value $r = 10^{B_{\text{dB}}/20}$. This last signal, $\mathbf{u}(t) \doteq u(t)e^{j\varphi(t)}$, is the input of a predistortion cubic device, characterized by an input-output relation of the type

$$\mathbf{v} \doteq v(t)e^{j\psi(t)} = \mathbf{u} \cdot (\mathbf{a} + \mathbf{b} \cdot u^2) \tag{5}$$

in which $\mathbf{a}$ and $\mathbf{b}$ are complex constants

$$\mathbf{a} \doteq \xi_1 + j\eta_1 \tag{5'}$$

$$\mathbf{b} \doteq \xi_2 + j\eta_2. \tag{5''}$$

The final amplifier (HPA) is supposed to give rise to the following instantaneous relation between the complex envelopes [1]

$$\mathbf{w} \doteq w(t)e^{j\theta(t)} = \mathbf{v}\frac{2}{1+v^2}e^{j\phi_0\frac{2v^2}{1+v^2}} \doteq \mathbf{q}(\mathbf{v}) \tag{6}$$

ϕ_0 being a constant which will be assumed to be equal to $\pi/6$.

To complete the analysis, in the block diagram of the transmitter, the presence of an RF filter is considered. Finally, the complex envelope of the transmitted signal is

$$\mathbf{s}(t) = \mathbf{q}(\mathbf{u}) * \mathbf{h}_T(t). \tag{7}$$

The idea, presented here, is to determine the characteristics of a predistorter which minimizes the total distortion power at the output of the HPA. By this way, the use of a transmission filter after the HPA can be avoided, and the dispersion of the received constellation, which is mainly due to the distortion component filtered by the group of filters after the HPA, can be reduced.

In order to determine $\mathbf{a}$ and $\mathbf{b}$, we define a reference predistorter, such that the overall transformation $\mathbf{u} \rightarrow \mathbf{w}$ is of the type [10], [11]

$$\mathbf{w} = \begin{cases} 2\mathbf{u} & \text{for } u < 1/2 \\ \frac{\mathbf{u}}{u} & \text{for } u \ge 1/2 \end{cases}. \tag{8}$$

Equation (8) shows that the reference predistorter completely eliminates the phase and amplitude distortion if $u < 1/2$ (i.e., $w < 1$), while, in the opposite case ($u \geq 1/2$), it gives rise to the saturation value of the HPA ($w = 1$). The input-output relation of the reference predistorter is thus given by

$$\mathbf{v} = \mathbf{f}(\mathbf{u}) = \begin{cases} \mathbf{u}\left\{\frac{1-\sqrt{1-(2u)^2}}{2u^2} e^{-j\phi_0[1-\sqrt{1-(2u)^2}]}\right\} & u < 1/2 \\ \frac{\mathbf{u}}{u} e^{-j\phi_0} & u \geq 1/2. \end{cases} \quad (9)$$

The method proposed can be expressed analytically by imposing that $\mathbf{a}$ and $\mathbf{b}$ be chosen in order to minimize the expected squared error derived from (5) instead of (9). The error at the HPA input can be expressed by

$$\mathbf{e}_v(\mathbf{u}) = \mathbf{f}(\mathbf{u}) - [\mathbf{u} \cdot (\mathbf{a} + \mathbf{b}u^2)] \quad (10)$$

and the error at the HPA output can be expressed by

$$\mathbf{e}_w(\mathbf{u}) = \begin{cases} 2\mathbf{u} - \mathbf{q}[\mathbf{u} \cdot (\mathbf{a} + \mathbf{b} \cdot u^2)] & u < 1/2 \\ \frac{\mathbf{u}}{u} - \mathbf{q}[\mathbf{u} \cdot (\mathbf{a} + \mathbf{b} \cdot u^2)] & u \geq 1/2. \end{cases} \quad (10')$$

If $p_{\mathbf{U}}(\mathbf{u}) = p_{\mathbf{U}}(u;\varphi)/u$ is the first order hierarchy of the process $\mathbf{U}(t)$ to which $\mathbf{u}(t)$ belongs, the expected squared value E_w^2 of the distortion introduced by the predistorter + HPA is

$$E_w^2 = \int_{u=0}^{r} \int_{\varphi=0}^{2\pi} |\mathbf{e}_w(ue^{j\varphi})|^2 p_{\mathbf{U}}(u;\varphi) du d\varphi \quad (11)$$

and the optimum $\mathbf{a}$ and $\mathbf{b}$ values are those for which (11) is minimum. However, this analysis does not lead to a solution which can be expressed in a closed form although obviously the realization of automatic adaptive algorithms for the predistorter coefficients is possible, as shown in Appendix 2. A closed form suboptimal solution, corresponding to the minimization of the expected squared error (11), before the HPA, will be determined. First, supposing that the random variables U and ϕ, with determinations u and φ, are independent, observing that, from (6) and (9), $|\mathbf{e}_v(\mathbf{u})|$ is a function of u only, and defining

$$\chi_0(u) + j\psi_0(u) \doteq \begin{cases} \frac{1}{2u}[1 - \sqrt{1-(2u)^2}] e^{-j\phi_0[1-\sqrt{1-(2u)^2}]} & u < 1/2 \\ e^{-j\phi_0} & u \geq 1/2 \end{cases}$$
$$\chi_1(u) = \psi_1(u) = u$$
$$\chi_2(u) = \psi_2(u) = u^3$$

one obtains, for the mean squared error E_v^2 of $\mathbf{e}_v(\mathbf{u})$

$$E_v^2 = E_\xi^2 + E_\eta^2 \quad (12)$$
$$E_\xi^2 \doteq \overline{\{\chi_0(u) - \xi_1\chi_1(u) - \xi_2\chi_2(u)\}^2}$$
$$E_\eta^2 \doteq \overline{\{\psi_0(u) - \eta_1\psi_1(u) - \eta_2\psi_2(u)\}^2}$$

in which ξ_1, ξ_2, η_1 and η_2 define $\mathbf{a}$ and $\mathbf{b}$ through (5′) and (5″). By using (12), it is then easy to obtain the system giving the suboptimal values of $\mathbf{a}$ and $\mathbf{b}$

$$\begin{cases} (\xi_1 \quad \xi_2) \cdot \mathbf{A}_\xi = \mathbf{B}_\xi \\ (\eta_1 \quad \eta_2) \cdot \mathbf{A}_\eta = \mathbf{B}_\eta \end{cases} \quad (13)$$

in which

$$\mathbf{A}_\xi = \begin{pmatrix} \phi_{11} & \phi_{12} \\ \phi_{21} & \phi_{22} \end{pmatrix} \quad \mathbf{A}_\eta = \begin{pmatrix} \Theta_{11} & \Theta_{12} \\ \Theta_{21} & \Theta_{22} \end{pmatrix}$$
$$\mathbf{B}_\xi = (\phi_{01} \quad \phi_{02}) \quad \mathbf{B}_\eta = (\Theta_{01} \quad \Theta_{02})$$
$$\phi_{ij} \doteq \overline{\chi_i(u)\chi_j(u)} \quad \Theta_{ij} \doteq \overline{\psi_i(u)\psi_j(u)}.$$

The suboptimal solutions for $\mathbf{a}$ and $\mathbf{b}$, given by (13), (5′) and (5″), are a function of the selected value for the input back-off, and define the MMSE predistorter. These solutions give values which are very close to the optimal ones (see Appendix 2).

The power spectral density and the total power of the undistorted and distorted components, at the HPA output, will now be determined. The complex envelope of the transmitted signal $\mathbf{s}(t)$ can be expressed as follows

$$\mathbf{s}(t) = \{\alpha \cdot 2\mathbf{u}_0(t) - \mathbf{e}_w[\mathbf{u}(t)]\} * \mathbf{h}_T(t) \doteq \mathbf{s}_U(t) + \mathbf{s}_d(t) \quad (14)$$

with average power $\mathcal{P}_{\mathbf{s}}$, and in which the undistorted component $\mathbf{s}_U(t)$ and the distortion component $\mathbf{s}_d(t)$ are introduced. These components are approximately orthogonal (they are orthogonal before the HPA, due to the way the constants $\mathbf{a}$ and $\mathbf{b}$ were defined), and it is meaningful to consider the powers separately. For simplicity, the transmission filter will be omitted in the following computations.

As regards the first component, one immediately has

$$\mathcal{P}_{\mathbf{s}_U} = 10^{\frac{C_{\mathrm{dB}}}{10}} \cdot F(\gamma, L) \quad (14')$$

where

$$F(\gamma, L) = \frac{\mathcal{P}_{\mathbf{U}_0}}{W_{U_0}}. \quad (14'')$$

$F(\gamma, L)$ can be interpreted as a *shape factor* of the signal $\mathbf{u}_0(t)$, since it is equal to the average power divided by the peak power, and

$$C_{\mathrm{dB}} \doteq 6 + B_{\mathrm{dB}}. \quad (14''')$$

C_{dB} can be interpreted as the output back-off, as is obvious by observing (8).

As regards the second component, the evaluation of the average power can be obtained by using (11) and numerical integration, after having determined the constants $\mathbf{a}$ and $\mathbf{b}$. The power spectral distribution is not easy to determine; the application of a simplified procedure (see Appendix 1) leads to the following approximate expression

$$\mathcal{P}_{\mathbf{s}_d}(f) \approx \frac{E_w^2}{2f_c}\left\{\mathrm{erfc}\left[\frac{f - 0.5f_c}{f_T}\right] - \mathrm{erfc}\left[\frac{f + 0.5f_c}{f_T}\right]\right\} \quad f > f_c \quad (14^{\mathrm{iv}})$$

where

$$f_T = f_c\sqrt{\frac{1.72(M+1)}{W_{\mathbf{U}_0}(M-1)}}. \quad (14^{\mathrm{v}})$$

B. Performance Evaluation

The performance evaluation consists in computing the symbol error probability P_e (as a function of the received signal to noise ratio and system parameters) and the system margin (as a function of the back-off and system parameters). Reference will be made to a QAM receiver. It is supposed that the radio channel does not introduce selective fading. Therefore, its behavior is described by a power attenuation A_d and a thermal noise. The complex envelope of the noise $\mathbf{n}(t) = n_c(t) + jn_s(t)$ is obtained by combining two realizations $n_c(t)$ and $n_s(t)$ belonging to two independent Gaussian processes with same bilateral uniform spectral density power, $\mathcal{N}_0$. The received signal can be expressed as [supposing, as previously, the absence of the transmission filter, see (14)]

$$\mathbf{r}(t) = A \cdot \mathbf{u}_0(t) B \mathbf{e}_w(t) + \mathbf{n}(t) \tag{15}$$

$$A = \sqrt{\frac{1}{A_d P_{\mathbf{U}_0}}} 10^{\frac{C_{\mathrm{dB}}}{20}} \quad B = -\sqrt{\frac{1}{A_d}}. \tag{16}$$

The front-end filter is supposed to realize, together with the transmission pulse shaper, a raised-cosine Nyquist characteristic; depending on the choice for $\mathbf{G}(f)$ according to (2) or (2′), one has

$$\mathbf{H}_R(f) = \begin{cases} \frac{1}{A} & |f| \le \frac{f_c}{2}(1+\gamma) \\ 0 & \text{elsewhere} \end{cases} \quad \text{[case A]} \tag{17′}$$

or

$$\mathbf{H}_R(f) = \begin{cases} \frac{1}{A}\sqrt{\mathbf{G}_\gamma(f)} & |f| \le \frac{f_c}{2}(1+\gamma) \\ 0 & \text{elsewhere} \end{cases} \quad \text{[case B].} \tag{17″}$$

Under these conditions, the demodulated signal $\mathbf{d}(t)$ is

$$\begin{aligned} \mathbf{d}(t) &= \mathbf{u}_0(t) * \mathbf{h}_R(t) + \frac{B}{A}\varepsilon_w(t) * \mathbf{h}_R(t) + \frac{1}{A}\mathbf{n}(t) * \mathbf{h}_R(t) \\ &\doteq \mathbf{d}_0(t) + \mathbf{d}_d(t) + \mathbf{d}_n(t) \end{aligned} \tag{18}$$

where the first component, $\mathbf{d}_0(t)$, is the undistorted signal expressed by

$$\mathbf{d}_0(t) = \mathbf{u}_0(t) * \mathbf{h}_R(t) = \sum_k \{x[k] + jy[k]\} \cdot g_\gamma(t - kT_c) \tag{19}$$

while the other two components, $\mathbf{d}_d(t)$ and $\mathbf{d}_n(t)$, represent the component due to non linear distortion

$$\mathbf{d}_d(t) \doteq \frac{B}{A}\mathbf{e}_w(t) * \mathbf{h}_R(t) \doteq \varepsilon_c(t) + j\varepsilon_s(t) \tag{20}$$

and the thermal noise contribution

$$\mathbf{d}_n(t) \doteq \frac{1}{A}\mathbf{n}(t) * \mathbf{h}_R(t) \doteq \nu_c(t) + j\nu_s(t). \tag{21}$$

In order to evaluate the performance of the system, two cases will be considered: the first, called *reference*, in which the predistorter is expressed by (9), and the second called *effective*, in which the MMSE predistorter is used. The evaluation will be determined analytically in the first case, and through simulation in the second case.

C. Performance Evaluation in the Reference Case

Under the hypothesis $C_{\mathrm{dB}} < 0$, the non linear distortion component is zero. Thus, $\mathcal{P}_{\mathbf{S}} = \mathcal{P}_{\mathbf{S}_U}$, the optimal sampling instants are equal to nT_c, and one has, at the sampler output

$$\begin{aligned} d_c[n] &= x[n] + \nu_c(nT_c) \\ d_s[k] &= y[n] + \nu_s(nT_c). \end{aligned} \tag{22}$$

Obviously, the presence of the equalizer is unnecessary.

In (22), $\nu_c = \nu_c(nT_c)$ and $\nu_s = \nu_s(nT_c)$ are determinations of independent Gaussian random variables, with an average value equal to zero and equal variance

$$\sigma^2 = \frac{1}{A^2}\mathcal{N}_0 \int_{-\infty}^{\infty} |\mathbf{H}_R(f)|^2 \, df. \tag{23}$$

A tight upper limit for the symbol error probability is expressed by

$$\begin{aligned} P_e &\lesssim \mathcal{P}_r\{|\nu_c| > 1/(M-1)\} + \mathcal{P}_r\{|\nu_s| > 1/(M-1)\} \\ &= 2\,\mathrm{erfc}\left\{\frac{1}{\sqrt{2}(M-1)\sigma}\right\}. \end{aligned} \tag{24}$$

From (23), it is possible to obtain the following expression for P_e

$$P_e = 2\ \mathrm{erfc}\{z\} \tag{25}$$

$$z^2 = \frac{\mathrm{SNR}}{\lambda(\gamma) \cdot \mu(L)} \tag{25′}$$

with

$$\lambda(\gamma) = \begin{cases} (1 - \gamma/4)(1+\gamma) & \text{(case A)} \\ 1 & \text{(case B)} \end{cases} \tag{26}$$

$$\mu(L) = 2[M(L)-1]^2 \mathcal{P}_C(L) \cong \frac{\pi}{3}[M^2(L) - 1] \tag{26′}$$

$$\mathrm{SNR} = \frac{\mathcal{P}_{\mathbf{S}}}{A_d \mathcal{P}_{\mathbf{N}}} \tag{26″}$$

[equivalent Signal to Noise ratio at the receiver]

$$\mathcal{P}_{\mathbf{N}} = \mathcal{N}_0 f_c \tag{26‴}$$

[Noise Power in a band equal to the symbol frequency].

Equation (25) gives an expression for P_e as a function of the normalized signal to noise ratio SNR. From (25), one can directly derive the margin of the reference system. If the probability of error must be lower than a given P_e, then the following inequalities, which are equivalent, must hold

$$z \ge \mathrm{erfc}^{-1}\{2 \cdot P_e\} \tag{27}$$

$$\mathrm{SNR} \ge [\mathrm{erfc}^{-1}(2P_e)]^2 \cdot \lambda(\gamma) \cdot \mu(L) \doteq \mathrm{SNR}_{\mathrm{ref}}(P_e, \gamma, L) \tag{27′}$$

$$\mathcal{P}_{\mathbf{S}} \ge A_d \mathcal{P}_{\mathbf{N}} \mathrm{SNR}_{\mathrm{ref}}(P_e, \gamma, L). \tag{27″}$$

Consequently, the system margin can be defined as

$$M_{\mathrm{ref}} \doteq \frac{\mathcal{P}_{\mathbf{S}}}{A_d \mathcal{P}_{\mathbf{N}} \mathrm{SNR}_{\mathrm{ref}}(P_e, \gamma, L)}.$$

From this expression, by using (14′)÷(14‴), one obtains

$$M_{\mathrm{ref}} = m_{\mathrm{ref}} 10^{\frac{C_{\mathrm{dB}}}{10}} \tag{28}$$

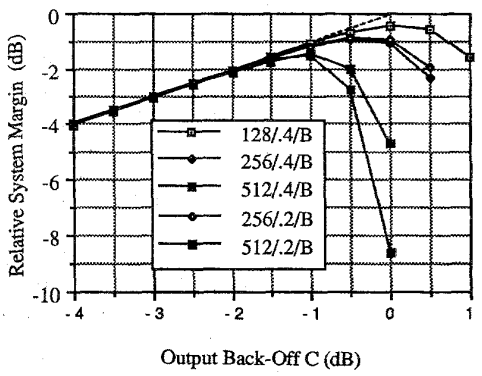

Fig. 2. In dotted lines: relative margin of the reference system $M_{\rm ref}/m_{\rm ref}$ as a function of the output back-off. Other curves: relative system margin as a function of the output back-off in the following cases: $L = 128$, $\gamma = 0.4$, case B [see (2″)], indicated on the figure as 128/0.4/B. $L = 256$, $\gamma = 0.4$, case B [see (2″)], indicated on the figure as 256/0.4/B. $L = 512$, $\gamma = 0.4$, case B [see (2″)], indicated on the figure as 512/0.4/B. $L = 256$, $\gamma = 0.2$, case B [see (2″)], indicated on the figure as 256/0.2/B. $L = 512$, $\gamma = 0.2$, case B [see (2″)], indicated on the figure as 512/0.2/B.

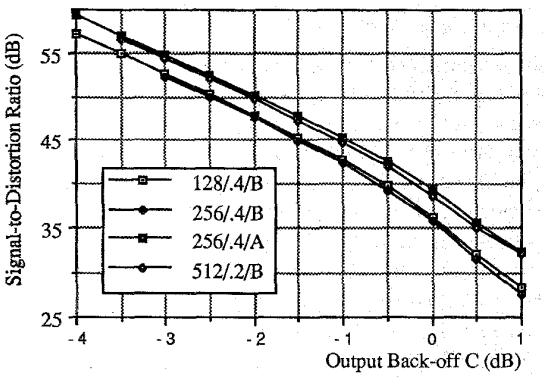

Fig. 3. Signal-to-distortion ratio as a function of the output back-off in the following cases: $L = 128$, $\gamma = 0.4$, case B [see (2″)], indicated on the figure as 128/0.4/B. $L = 256$, $\gamma = 0.4$, case B [see (2″)], indicated on the figure as 256/0.4/B. $L = 256$, $\gamma = 0.4$, case A [see (2)], indicated on the figure as 256/0.4/A. $L = 512$, $\gamma = 0.2$, case B [see (2″)], indicated on the figure as 512/0.2/B.

where

$$m_{\rm ref} = m_{\rm ref}(P_e, \gamma, L) = \frac{F(\gamma; L)}{A_d \mathcal{P}_{\rm N} {\rm SNR}_{\rm ref}(P_e, \gamma, L)}. \quad (29)$$

Fig. 2 (dotted line) shows the behavior of the relative margin of the reference system $M_{\rm ref}/m_{\rm ref}$ expressed in dB, as a function of the output back-off.

D. Performance Evaluation in the Effective Case

A simulation program, described in [12] and [13], was used in order to evaluate the performance of the system in the effective case. It can simulate the transmission of a multilevel pseudo-random periodic sequence with period N (N multiple of 2) . For the results shown in the present paper, values for N, between 1024 and 8192, were considered. Following a suggestion made by one of our reviewers, all the results obtained were verified considering sequences which were twice as long. Variations in the results obtained were lower than 0.55 dB. The program allows the introduction of a pair of adjacent channels, having assigned spectral distance and attenuation, and takes into account an optimum MMSE tapped-line equalizer, with a length of $2H + 1$, located after the sampler.

Preliminary parameters, such as the signal power at the HPA output $\mathcal{P}_S = \mathcal{P}_S(C_{\rm db}, \gamma, L)$, the shape factor $F = F(\gamma, L)$ and the first order hierarchy of the amplitude of the signal $\mathbf{u}_0(t)$, can be estimated by using the simulation program.

In addition, using $p_{U_0}(u_0)$, it is possible to evaluate the first order hierarchy of $u(t)$ and, thus, the expected values (12), and the optimum $\mathbf{a}$ and $\mathbf{b}$ values through (5′), (5″), and (13). Fig. 3 shows the signal to distortion ratio at the HPA output computed with $\mathbf{a}$ and $\mathbf{b}$ optimal values. Note that the criterion gives rise to a non linear distortion value which is very satisfactory: this is confirmed by the data of Fig. 4, showing an example of the power spectral densities of the signal at the HPA output as a function of the output back-off. Indeed, the power outside the band is small, making the presence of transmission filters unnecessary, even for output back-off values close to 0 dB.

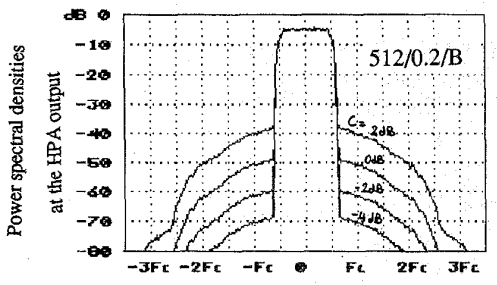

Fig. 4. Power spectral densities of the signal at the HPA output for various output back-off values ($C = 2, 0, -2, -4$ dB, as indicated on the curves), and in the $L = 512/\gamma = 0.2$/case B configuration.

The simulation program also allows the estimation of $P_e = P_e\{z\}$, with z given by (25′) or of its inverse function

$${\rm SNR} = z^2(P_e) \cdot \lambda(\gamma) \cdot \mu(L) \doteq {\rm SNR}(P_e, \gamma, L, C_{\rm dB}). \quad (30)$$

Fig. 5 shows the behavior of the degradation of the signal to noise ratio $\{{\rm SNR}()/{\rm SNR}_{\rm ref}()\}$ for some γ and L values, and for $P_e = 10^{-4}$, as a function of the output back-off. Note that the degradation of SNR is quite low, showing a small scattering of the values in the received constellation. This degradation is always higher in case B than in case A (the example of 256 levels is shown in Fig. 5), confirming that the instantaneous non linearity produces noticeable effects, especially if followed by significant filtering.

Finally, the evaluation of the function $\mathcal{P}_S(C_{\rm dB}, \gamma, L)$ allows the evaluation of the system margin

$$M \doteq \frac{\mathcal{P}_{\rm S}(C_{\rm dB}, \gamma, L)}{A_d \mathcal{P}_{\rm N} {\rm SNR}(P_e, \gamma, L, C_{\rm dB})}$$

and of the relative system margin

$$M_R = \frac{M}{m_{\rm ref}} = \frac{\mathcal{P}_{\rm S}(C_{\rm dB}, \gamma, L)}{F(\gamma, L)} \cdot \frac{{\rm SNR}_{\rm ref}(P_e, \gamma, L)}{{\rm SNR}(P_e, \gamma, L, C_{\rm dB})}. \quad (31)$$

Fig. 2 shows the relative system margin as a function of the output back-off, for some γ and L values, in case B.

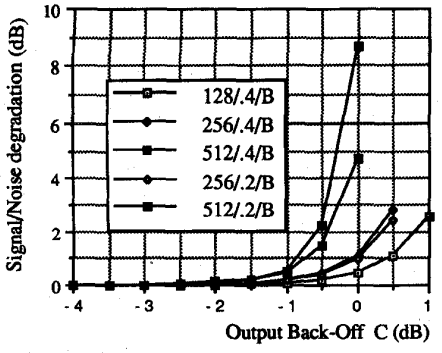

Fig. 5. Signal-to-noise degradation, as a function of the output back-off, in different cases as indicated on the figure according to the standard explained for the preceding figures.

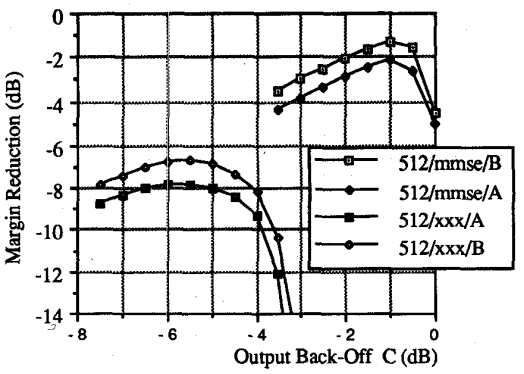

Fig. 6. Margin reduction as a function of the output back-off in the following cases: $L = 512$, MMSE predistorter, case B [see (2″)], indicated on the figure as 512/mmse/B. $L = 512$, predistorter described in [7], case B [see (2″)], indicated on the figure as 512/xxx/B.

Note that the MMSE predistorter has a similar behavior to the reference predistorter, and gives rise to a degradation of the system margin ranging between 0.5 and 1.5 dB.

III. Application to 512 QAM Systems

In this section, the effect of the MMSE predistorter on a 2 × 155 Mb/s system, with channel spacing of 40 MHz with alternating polarization and symbol frequency $f_c = 34.44$ Mbaud, will be analyzed. The transmission filter RF will not be considered. The crosspolarization attenuation is 18 dB. It will be supposed that the overall system filtering is of Nyquist raised-cosine type, equally shared between emitter and receiver, with $\gamma = 0.16$.

Degradations due to a non ideal receiver (sampling jitter, phase error in the carrier) will not be considered, but attention will be focused on the amount of margin reduction due to the HPA and on the determination, through the signature, of the system sensitivity to multipath [14], [15].

A. Evaluation of the Margin Reduction Due to the Combination of MMSE Predistorter and HPA

The margin reduction can be evaluated by estimating the entities which appear in (30) and considering the presence of adjacent channels with orthogonal polarization. Fig. 6 shows the behavior of the relative margin as a function of the output back-off, compared to similar behaviors obtained with the predistorter described in [7]. These results show an excellent behavior of the MMSE predistorter which can be quantified by an improvement of about 5 dB.

B. Evaluation of the Sensitivity of the System to Multipath

Multipath propagation can be taken into account by a *3 paths model* [16], [17]. This corresponds to the introduction of an additional transfer function characterized as

$$\mathbf{C}(f) = a[1 - (1-\mu)e^{j\phi}e^{-j2\pi f\tau}] \equiv \mathbf{C}(0) \cdot \mathbf{C}_0(f). \quad (32)$$

τ is assumed to be equal to 6.3 ns, while a, μ and ϕ must be considered, at a particular time when multiple paths are present, as determinations of random variables [17]. In particular, the term in the squared parenthesis of (32) corresponds to a selective behavior in frequency but a unitary gain at $f = 0$, with a minimum value equal to μ at frequency $f_b = \phi/2\pi\tau$.

When $a = \mu = 1$, the model (32) describes the absence of multipath. In the other cases, the presence of multipath is effective and gives rise to two effects.

The first effect is that $\mathbf{C}(0)$ is not usually unitary, and implies a change in the received power equal to $|\mathbf{C}(0)|^2$. The second effect is that a new value of SNR, called SNR′, is required for obtaining a given P_e; this value depends upon $\mathbf{C}_0(f)$ and upon ϕ and μ, but not on a. The two effects combine and the new system margin becomes

$$M' = M\frac{\mathrm{SNR}(P_e, \gamma, L, C_{\mathrm{dB}})}{\mathrm{SNR}'(P_e, \gamma, L, C_{\mathrm{dB}})}|\mathbf{C}(0)|^2. \quad (33)$$

Under these conditions, a function, which well represents the system sensitivity to multipath, is the signature of the system, defined by the points (a, μ, ϕ) for which the system margin, in dB, is equal to zero; this set of points is a family of curves in the plane $(\mu_{\mathrm{dB}} = -10\log_{10}\mu^2, \phi)$ with parameter $a_{\mathrm{dB}} = -10\log_{10}a^2$.

Without equalization, the predominant effect of the model (32) is that it generates intersymbol interference. In the range of M and a_{dB} values of practical interest, the system signature can be simply evaluated as the set of points $(\mu_{\mathrm{dB}}, \phi)$ insensitive to a_{dB} which produce a closure of the eye diagram using a peak distortion criterion. Under these conditions, and using the MMSE predistorter, it can be verified by simulation that the system signature is almost independent of the output back-off, when less than ≈ -1 dB, and has the shape of Fig. 7, case 4. In addition, this figure shows the system signature when a three taps equalizer is used for $L = 512$, 256, and 128. In all cases the output back-off is -3 dB.

The absence of an equalizer is only a theoretical situation, due to the high percentage of outage time which it originates. The other extreme case is perfect equalization, in order to completely eliminate the intersymbol interference produced by $\mathbf{C}_0(f)$. The behavior of this equalizer, called reciprocal equalizer, is well described in the literature (see for example [18]). It gives rise to a transfer function equal to the inverse of $\mathbf{C}_0(f)$ and its final effect is to change the thermal noise power in the decision point. In this case, SNR′ is related to

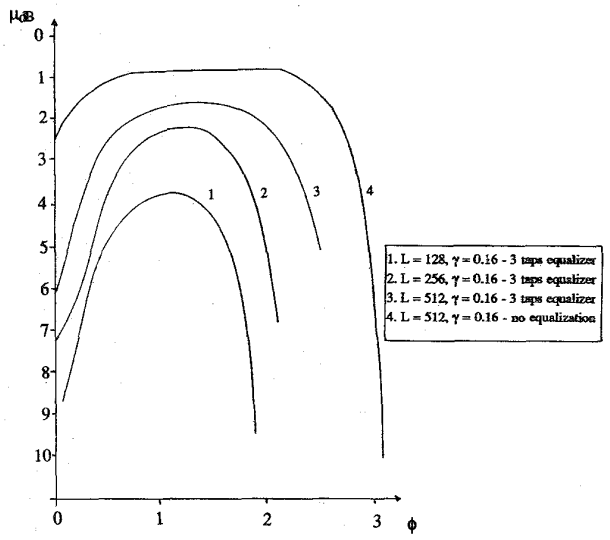

Fig. 7. System signature evaluated as the set of points $(\mu_{\mathrm{dB}}, \phi)$ which produce a closure of the eye diagram. The four curves labeled 1., 2., 3., and 4., correspond to the following cases: 1. $L = 128$, $\gamma = 0.16$—3 taps equalizer. 2. $L = 256$, $\gamma = 0.16$—3 taps equalizer. 3. $L = 512$,$\gamma = 0.16$—3 taps equalizer. 4. $L = 512$, $\gamma = 0.16$—no equalization.

SNR by the equation

$$\mathrm{SNR}' = \mathrm{SNR} \cdot f(\mu_{\mathrm{dB}}, \phi, \gamma) \tag{34}$$

in which

$$f(\mu_{\mathrm{dB}}, \phi, \gamma) = \frac{\int \{|\mathbf{H}_R(f)|^2 / |\mathbf{C}_0(f)|^2 df}{\int |\mathbf{H}_R(f)|^2 df}$$

and using (32), (33) and (34) it is possible to deduce that the system signature is the set of points in the plane (μ, ϕ), with parameter a_{dB}, which satisfies the relation

$$g_{\mathrm{dB}}(\mu, \phi, \gamma) = M_{-\,\mathrm{dB}} - a_{\mathrm{dB}} \tag{35}$$

with

$$g_{\mathrm{dB}}(\mu, \phi, \gamma) = 10 log_{10} g(\mu, \phi, \gamma) \tag{36}$$

and

$$\begin{aligned} g(\mu, \phi, \gamma) &= \frac{\int_{-B}^{B} |\mathbf{H}_R(f)|^2 df / |1 - (1-\mu)\exp\{j(\phi - 2\pi f \tau)\}|^2}{\int_{-B}^{B} |\mathbf{H}_R(f)|^2 df} \\ &= g(\mu, -\phi, \gamma) \\ B &= \frac{1}{2} f_c (1 + \gamma). \end{aligned} \tag{37}$$

In this case, the system signature (an example when $M_{\mathrm{dB}} = 30$ and $\gamma = 0$ is given in Fig. 8) depends only upon the nominal margin M and not upon the single parameters which define the system except for the influence of the roll-off γ which, since we suppose a perfect synchronization in the receiver, is low. In other words, the presence of the HPA and of the predistorter, influences only indirectly the signature, through a margin reduction introduced by the HPA + predistorter. Under this point of view, the proposed predistorter operates in a very satisfactory way, since it gives rise to a modest margin reduction.

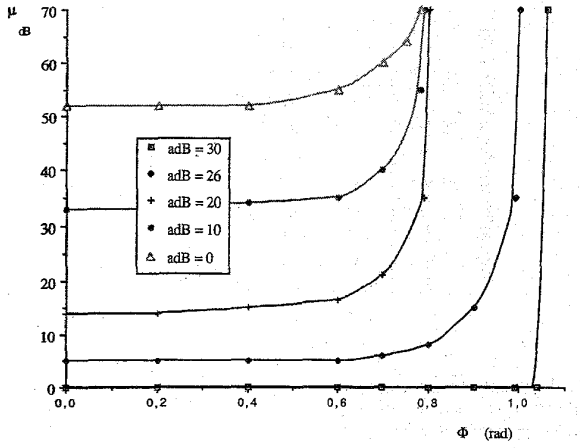

Fig. 8. Signature of the system as a function of a_{dB}, in the case of perfect equalization, $M_{\mathrm{dB}} = 30$, and $\gamma = 0$.

IV. Conclusion

In this paper, a new procedure for the determination of an analog predistorter used for compensating the effects of the nonlinearities introduced by HPA in digital transmission systems with very high spectral efficiency, is proposed. Margin losses lower than ~1.5 dB are obtained, also in the case of systems with a spectral efficiency of 7.75 bit/Hz, which require 512 points constellations and low roll-off values. Finally, the influence of multipath is discussed, by examining the influence of the nonlinearities introduced by the HPA and the predistorter on the system signature, in the two extreme cases of absence of equalization and of equalization, obtained with a reciprocal equalizer.

Appendix 1
Evaluation of the Power Spectral Density of the Distortion of the Residual Non Linearity

In this appendix, an approximate evaluation of the power spectral density of the distortion term $\mathbf{e}_w(t)$ will be described.

For this purpose, observe that, from (5), v^2 can be expressed in terms of u

$$v^2 = u^2 |\mathbf{a} + \mathbf{b}u^2| \doteq p(u)$$

and thus, using (6) in (10′)

$$\begin{aligned} \mathbf{e}_w(\mathbf{u}) &= 2\mathbf{u} - \mathbf{u}(\mathbf{a} + \mathbf{b}u^2) \cdot \frac{2}{1 + p(u)} \exp\left\{ j\phi_0 \frac{2p(u)}{1 + p(u)} \right\} \\ &\doteq \mathbf{u} \cdot \mathbf{q}(u) = \alpha \mathbf{u}_0 \cdot \mathbf{q}(u). \end{aligned} \tag{A.1}$$

In the previous equation, the function $\mathbf{q}(u) = \mathbf{q}[u(t)]$ is better represented by the Fourier series, rather than by a power series. Therefore, it can be stated that (recalling that $r = \max_t |u(t)|$)

$$\mathbf{q}(u) = \sum_n \mathbf{Q}_n \cos\left(\frac{\pi n u}{r} + \phi_n\right) \approx \mathbf{Q}_1 \cos\left(\frac{\pi u}{r} + \phi_1\right)$$

in which the first term of the series is considered, and the mixed moment of order (1, 1) of $\mathbf{q}[u(t)]$ is

$$m_{\mathbf{Q}}^{(1,1)}(\tau) = |\mathbf{Q}_1|^2 \overline{\cos\left[\frac{\pi u(t)}{r} + \phi_1\right] \cos\left[\frac{\pi}{r} u(t+\tau) + \phi_1\right]}. \tag{A.2}$$

Now, for $\tau \to 0$:

$$\cos\left(\frac{\pi}{r}u(t+\tau)+\phi_1\right) \cong \cos\left(\frac{\pi}{r}u(t)+\phi_1\right) + \frac{\pi}{r}u(t)\sin\left(\frac{\pi}{r}u(t)+\phi_1\right) + \left[\frac{\pi}{r}\ddot{u}(t)\sin\left(\frac{\pi}{r}u(t)+\phi_1\right) + \frac{\pi^2}{r^2}\dot{u}(t)^2\cos\left(\frac{\pi}{r}u(t)+\phi_1\right)\right]\frac{1}{2}\tau^2+\cdots$$

and remembering that $u(t)$ and $\dot{u}(t)$ are orthogonal, the following equation can be obtained

$$m_{\mathbf{Q}}^{(1,1)}(\tau) \cong \overline{\cos^2\left[\frac{\pi}{r}u(t)+\phi_1\right]}|\mathbf{Q}_1|^2\left[1-\frac{1}{2}\frac{\pi^2}{r^2}\overline{\dot{u}(t)^2}\tau^2\right] \cong A^2 e^{-\frac{1}{2}\frac{\pi^2}{r^2}\overline{\dot{u}(t)^2}\tau^2}$$

$$A^2 \doteq \overline{\cos^2\left[\frac{\pi}{r}u(t)+\phi_1\right]}|\mathbf{Q}_1|^2 \quad (\tau \to 0). \tag{A.3}$$

In addition, for $\tau \to \infty$, it can be assumed that $m_Q^{(1.1)}(\tau)$ tends to zero, and the previous approximation can be considered as valid for any τ. Therefore, it can be deduced, by taking the Fourier transform of (A.3), that the power spectral density of $\mathbf{q}[u(t)]$ is expressed by

$$\mathcal{P}_{\mathbf{Q}}(f) \approx A^2 e^{-f^2/f_T^2} \equiv \frac{\mathcal{P}_{\mathbf{Q}}}{\sqrt{\pi}f_T}e^{-f^2/f_T^2} \quad \{\mathcal{P}_{\mathbf{Q}} = \text{Mean Power of } \mathbf{q}[u(t)]\} \tag{A.4}$$

with

$$f_T^2 = \frac{1}{2r^2}\overline{\dot{u}(t)^2} = \frac{1}{2r^2}\int_{-0.5f_c(1+\gamma)}^{0.5f_c(1+\gamma)} 4\pi^2 f^2 2\alpha^2 \mathcal{P}_c \frac{|\boldsymbol{G}_\gamma(f)|^2}{f_c}df \approx \frac{1.72}{W_{U_0}}\frac{M+1}{M-1}f_c^2$$

[in the preceding expressions, (4), (4′), (4″) are used and it is supposed that $\gamma = 0$].

Finally, supposing that $\mathbf{u}(t)$ is independent of $\mathbf{q}[u(t)]$, one has, from (A.1) and (A.4)

$$\mathcal{P}_{\mathbf{e}_w}(f) = \alpha^2\mathcal{P}_{\mathbf{U}_0}(f) * \mathcal{P}_{\mathbf{Q}}(f) = \frac{\alpha^2\cdot\mathcal{P}_c}{f_c}\int_{-0.5f_c}^{0.5f_c}\mathcal{P}_{\mathbf{Q}}(f-\xi)d\xi = \frac{\alpha^2\mathcal{P}_c\mathcal{P}_{\mathbf{Q}}}{2f_c}\cdot\frac{2}{\sqrt{\pi}}\int_{-0.5f_c}^{0.5f_c} e^{-\frac{(f-\xi)^2}{f_T^2}}d\xi$$

from which it is easy to deduce (14^{iv}) if one notes that, under the hypothesis that $\gamma = 0$ and that $\mathbf{u}(t)$ be independent of $\mathbf{q}[u(t)]$, one has, from (A.1), $E_w = \mathcal{P}_U \cdot \mathcal{P}_{\mathbf{Q}} = \alpha^2\mathcal{P}_c \cdot \mathcal{P}_{\mathbf{Q}}$.

Appendix 2
Adaptation of the Coefficients of the Cubic Predistorter of Section II

In this Appendix, on the basis of the optimal criterion described in Section II, a possible scheme for the adaptation of the predistorter coefficients will be presented, and its feasibility will be proved. In the following, no effort was made to simplify the adaptation algorithm since this would be beyond the aims of the present paper, also considering that the convergency rate is not a critical factor in common applications (as for example in back-off control, temperature variations and aging compensation).

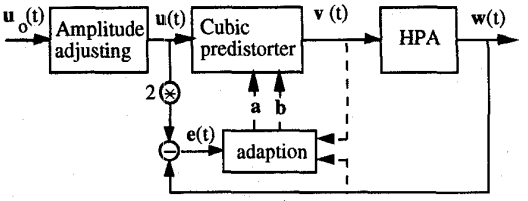

Fig. 9. General scheme of a system with adaptive cubic predistortion.

Starting from (10′), the scheme for a cubic adaptive predistorter is shown on Fig. 9, in which the module "Adaption" receives the error, together with the inputs and outputs of the predistorter (when needed), and computes the values of the coefficients of the predistorter. If ω is a generic real coefficient of the predistorter, a well known iterative relation which allows convergence of its value to the one which minimizes the mean squared error, as requested by the optimal criterion proposed in Section II, is the following

$$\omega_n = \omega_{n-1} - \gamma\frac{\partial|\mathbf{e}|^2}{\partial\omega}\bigg|_{t=nT} \tag{A2.1}$$

in which n is the iterative index, $1/T$ is the updating frequency and γ is a constant which is opportunely small for stability reasons. One can apply for simplicity the preceding expression to the adaptation of only $\mathbf{b} = \xi_2 + j\cdot\eta_2$. To this aim, one must compute the derivatives of $|\mathbf{e}|^2$ with respect to ξ_2 and η_2; setting $x = v^2$, one obtains

$$\frac{\partial|\mathbf{e}|^2}{\partial\xi_2} = 8u^4(\xi_1+u^2\xi_2)\left[1-\mathbf{Re}\left\{\frac{\mathbf{u}^*\mathbf{w}(1+x^2)}{2x}\times\left[1+j\left(4\phi_0\frac{x}{1-x^2}-\frac{1+x}{1-x}\frac{\eta_1+u^2\eta_2}{\xi_1+u^2\xi_2}\right)\right]\right\}\right]$$

$$\frac{\partial|\mathbf{e}|^2}{\partial\eta_2} = 8u^4(\eta_1+u^2\eta_2)\left[1-\mathbf{Re}\left\{\frac{\mathbf{u}^*\mathbf{w}(1+x^2)}{2x}\times\left[1+j\left(4\phi_0\frac{x}{1-x^2}-\frac{1+x}{1-x}\frac{\xi_1+u^2\xi_2}{\eta_1+u^2\eta_2}\right)\right]\right\}\right]. \tag{A2.2}$$

Convergency trials showed that although the γ parameter was not optimized, 10 000 iterations are sufficient for $\mathbf{b}$ to reach a new optimal value. As a typical example, for a 512 QAM system with input back-off $= -7$ dB, $\gamma = 0.3$, and optimal shaping, when $\mathbf{a} = 0.985 + j\cdot 0.025$, the obtained b value from (A2.2) is $\mathbf{b} = 1.40 - j\cdot 1.66$, while the sub-optimum value from theory of Section II is $\mathbf{b} = 1.41 - 1.65j$.

References

[1] A. A. Saleh, "Frequency-independent and frequency-dependent non linear models of TWT amplifiers," *IEEE Trans. Commun.*, vol. COM-29, no. 11, pp. 1715–1720, Nov. 1981.

[2] A. A. M. Saleh and J. Salz, "Adaptive linearization of power amplifiers in digital radio systems," *B.S.T.J.*, vol. 62, no. 4, pp. 1019–1033, Apr. 1983.

[3] K. S. Shanmugan and M. J. Ruggles, "An adaptive linearizer for 16-QAM transmission over nonlinear satellite channels," in *Proc. GLOBECOM '86*, Dec. 1–4, 1986, Houston, TX, Paper 4.3.1, pp. 0126–0130.

[4] M. F. Mesiya, P. McLane, and L. L. Campbell, "Maximum likelihood sequence estimation of binary sequences transmitted over bandlimited nonlinear channels," *IEEE Trans. Commun.*, vol. COM-25, pp. 633–643, July 1977.
[5] S. Benedetto and E. Biglieri, "Non linear equalization of digital satellite channels," *IEEE J. Select. Areas Commun.*, vol. SAC-1, pp. 57–62, Jan. 1983.
[6] J. Namiki, "An automatically controlled predistorter for multilevel quadrature amplitude modulation," *IEEE Trans. Commun.*, vol. COM-31, no. 5, pp. 707–712, May 1983.
[7] S. Pupolin and L. J. Greenstein, "Performance analysis of digital radio links with non linear transmit amplifiers," *IEEE J. Select. Areas Commun.*, vol. SAC-5, no. 3, pp. 534–546, Apr. 1987.
[8] T. Nojima, T. Murase, and N. Imai, "The design of a predistortion linearization circuit for high-level modulation radio systems," in *Proc. GLOBECOM '85*, Dec. 2–5, 1985, New Orleans, LA, Paper 47.4.1, pp. 1466–1471.
[9] K. Takeda, N. Lizuka, Y. Daido, S. Takenaka, and H. Nakamura, "Performance of 256 QAM modem for digital radio system," in *GLOBECOM '85*, Dec. 2–5, 1985, Paper 47.2, pp. 1455–1459.
[10] P. Hetrakul and D. P. Raylor, "Compensators for bandpass nonlinearities in satellite communications," *IEEE Trans. Aeros. Electron. Syst.*, vol. AES-12, pp. 509–514, July 1976.
[11] X. T. Vuong and H. J. Moody, "Realization of predistortion compensators of memoryless nonlinear devices," in *ICC '80*, pp. 33.7.1–33.7.5, 1980.
[12] G. Jacovitti and P. Mandarini, "Simulazione ibrida di sistemi di trasmissione numerici," *Alta Frequenza*, vol. XLVI, no. 5, 1977.
[13] T. D'Alessio and G. Jacovitti, "Stima di spettri di segnali numerici mediante simulazione," *Alta Frequenza*, vol. XLVII, no. 6, 1978.
[14] A. J. Giger and W. T. Barnett, "Effect of multipath propagation on digital radio," *IEEE Trans. Commun.*, vol. 29, no. 9, pp. 1345–1352, Sept. 1981.
[15] C. W. Lundgren and W. D. Rummler, "Digital radio outage due to selective fading-observation vs. prediction from laboratory simulation," *BSTJ*, pp. 1073–1100, May–June 1979.
[16] W. D. Rummler, "A new selective fading model: Application to propagation data," *BSTJ*, vol. 58, pp. 1037–1071, May–June 1979.
[17] ——, "More on the multipath fading channel model," *IEEE Trans. Commun.*, vol. 60, pp. 193–214, Feb. 1981.
[18] W. C. Wong and L. J. Greenstein, "Multipath fading and adaptive equalizers in microwave digital radio," *IEEE Trans. Commun.*, vol. COM-32, no. 8, pp. 928–934, Aug. 1984.
[19] S. Pupolin, A. Sarti, and H. Fu, "Performance analysis of digital radio links with nonlinear transmit amplifier and data predistorter with memory," in *ICC '89*, pp. 0292–0296, 1989.
[20] G. Karam and H. Sari, "Data predistortion techniques using intersymbol interpolation," *IEEE Trans. Commun.*, vol. 38, no. 10, pp. 1716–1723, Oct. 1990.
[21] ——, "A data predistortion technique with memory for QAM radio systems," *IEEE Trans. Commun.*, vol. 39, no. 2, pp. 336–344, Feb. 1991.

Maria-Gabriella Di Benedetto (M'89–SM'93) was born in Naples, Italy, in 1958. She obtained her "Laurea" in electrical engineering from the University of Rome 'La Sapienza' in 1981, magna cum laude *and publication of her thesis*. She went on to specialize in control systems engineering (1983) and earned her "Dottore di Ricerca" (Ph.D.) in electrical communications also from the University of Rome 'La Sapienza' in 1987.

Her professional positions have included numerous Fellowships and Associate professorships—she is presently an Associate Professor of Electrical Communications at the University of Rome 'La Sapienza'—and various visiting positions, at Massachusetts Institute of Technology (Cambridge, USA), and University of California at Berkeley (USA). In 1994, she received the Mac Kay Professorship academic award, at the University of California at Berkeley (USA). Her research interests include speech analysis and synthesis, and digital communication systems.

Dr. Di Benedetto is a member of the European Speech Communication Association (ESCA), and of the New York Academy of Sciences.

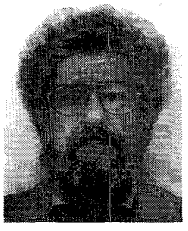

Paolo Mandarini was born in Rome in 1940. He received his "Laurea" degree in electronic engineering from the University of Rome, in 1963.

From 1965 to 1971, he was a Research Fellow of the Fondazione Ugo Bordoni, in Rome. In 1971, he joined INFOCOM Department of the University of Rome 'La Sapienza', where he is currently Full Professor of Electrical Communications. Professor Mandarini's research activities are in the field of signal theory, detection theory and related topics, with emphasis in digital communications and speech analysis.